applied sciences

MDPI

Article

Flexural Vibration Analysis of Nuclear Fuel Rod Bundles Interacting with Surrounding Fluid Subjected to Pressure Wave

Wonseok Yang [1], Heungseok Kang [2] and Junhong Park [3,*]

[1] Department of Automotive Engineering, Korea National University of Transportation, Chungju 27469, Korea; wsyang@ut.ac.kr
[2] ATF Technology Development Department. Korea Atomic Energy Research Institute, Daejeon 34057, Korea; hskang@kaeri.re.kr
[3] Department of Mechanical Engineering, Hanyang University, Seoul 04763, Korea
* Correspondence: parkj@hanyang.ac.kr; Tel.: +82-2-2220-0424

Received: 4 February 2020; Accepted: 20 March 2020; Published: 27 March 2020

Featured Application: This approach allows vibration analysis of the nuclear rod bundles with surrounding fluid using the spectral element method.

Abstract: The structural behavior of the nuclear rod bundles that consisted of cylindrical beams was predicted using the spectral element method (SEM) while considering the interaction with the surrounding fluid. Viscous fluid behavior was utilized in order to calculate the forces acting on the nuclear rod bundles from the incident pressure waves. The added mass and fluid coupling on the nuclear rod bundles were determined for the position patterns and gaps of each of the cylindrical beams. The pressure field from propagating waves in the surrounding fluid was calculated with respect to the boundary conditions of the surface of the vibrating structures. With the increasing number of nuclear rods and decreasing pressure wavelengths, the structural vibration of the nuclear rod bundles that were induced by the propagating forces affected the scattering events of the pressure field. The frequency response of the nuclear rod bundles from the pressure waves in the water exhibited smaller damping, because the incident pressure wave travels without fluid coupling due to the longer wavelength when compared with distance between rods. The proposed numerical method can be utilized for the detailed design for effective parameters of a supporting system to reduce the vibration of nuclear fuel rod bundles for safety control.

Keywords: fuel rod bundles; vibration; fluid coupling; SEM

1. Introduction

The structural instability that was induced by pressure pulsation and external force in nuclear power reactors, fuel pumps, air conditioning systems, and heat exchanger tubes has received increasing attention in recent years [1–6]. Nuclear fuel rod bundles that were exposed to coolant flow should be protected from structural failure [7]. The vibrations are affected by the instability of the fluid flow through the pipe system. It is necessary to analyze the motion of the nuclear rod bundles induced by fluid flow and design the support system that has large damping and stiffness to protect the nuclear rod bundles subjected to instability [8]. To simulate the behavior of nuclear rod bundles induced by fluid flow, coupling of the fluid flow and structural vibration is required. The fluid–structure interaction analysis was performed while using the following procedures. Structural deformation occurs due to fluid force; as the structure deforms, the pressure magnitude of the surrounding fluid and its direction to the flow change, and this induces changes in the pressure fields. Consequently, the changed pressure

fields act on the structure. A numerical analysis in the time domain was developed to analyze the interaction between the fluid and structure. The development of a numerical solution in the frequency domain is required for parametric studies to analyze the damping performance because the transient analysis requires a significant amount of computation time for accuracy.

Fluid–structure interaction was solved using the finite element method [9–11]. The structural vibration of a liquid-filled pipe system was analyzed while considering the extended water hammer equations using a polynomial function [9,10]. The shape function using non-uniform rational B-splines was used to increase the accuracy of the numerical results [11]. Because conventional finite element models are expressed by frequency-independent polynomial shape functions, the configuration of the model influences the accuracy in the high frequency modes of interest [12–14]. SEM using a shape function was developed to increase the accuracy of the numerical analysis [15–19]. The structural vibration of the pipelines conveying internal steady flow was simulated after considering the interaction with longitudinal and flexural vibrations. The momentum conservation for fluid flow in a pipe system and the governing equation of the vibration for pipelines conveying internal steady flow was analyzed using SEM [15]. Additionally, the flexural vibration of the pipeline considered the unsteady flow [16]. The behavior of blood flow, such as the viscoelastic nature of blood vessels, was analyzed using SEM [17]. The blood flow rate and pressure calculated by SEM was accurately more than those of the finite element method. In petroleum engineering applications, the effects on axial force, annulus fluid properties, and geometry for a braced well have been thoroughly investigated [18,19]. Viscous coupling for each structure in the fluid medium was not considered when the structural vibration of nuclear rod bundles interacting with the surrounding fluid was simulated.

There has been limited research regarding the numerical analysis of the structural behavior of nuclear rod bundles that were subjected to viscous fluid for the consideration of the supporting system. It is difficult to consider the viscous fluid coupling effects, because CFD analysis requires a large amount of computation time for accuracy and difficult numerical methods. Most studies focused on the simulation without the influence of hydrodynamic fluid coupling of each structure due to the computation time. The development of a new numerical method for calculating the vibration of nuclear rod bundles in viscous fluid for the design of support systems is necessary.

This study simulated the flexural vibration of the nuclear rod bundles interacting with viscous fluid using SEM based on the wave approach. The nuclear rod bundles consisted of 25 cylindrical beams, as shown in Figure 1. The added mass and viscous damping of the surrounding fluid on the structure were analyzed by the viscosity theory. The pressure force applied to each cylindrical beam was calculated while using the scattering wave solution of the surrounding fluid. The flexural vibration of the single nuclear rod induced by point force was simulated and the transient decay of displacement was confirmed in order to investigate the viscous damping of the surrounding fluid. With the plane sound wave incident on the nuclear rod bundles, the flexural displacement and phases of each cylindrical beam was calculated to investigate the characteristics of viscoelastic damping.

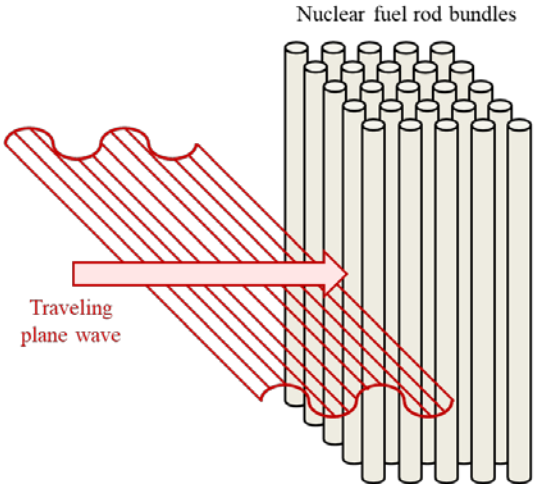

Figure 1. Flexural vibration of nuclear fuel rod bundles subjected to traveling plane wave caused by external collisions.

2. Equation of Motion for Nuclear Rod Bundles Surrounded by Viscous Fluid

2.1. Flexural Vibration of Nuclear Rod Bundles

The nuclear rod bundles were assumed to be cylindrical beams, as shown in Figure 2. The flexural vibration for the i–th cylinder was obtained, as

$$EI\frac{\partial^4 w_i}{\partial x^4} + \rho_s A_s \frac{\partial^2 w_i}{\partial t^2} = F_{v,i} + F_{p,i} \tag{1}$$

where E is Young's modulus, I is the inertia, ρ_s is the mass density, A_s is the cross-sectional area, and i ranges from 1 to N. F_v is the viscous hydrodynamic force induced by the presence of fluid, and F_p is the external force that is caused by the propagating pressure waves. The viscous hydrodynamic force was determined by the density and damping of the fluid. The hydrodynamic forces analyzed the effect of the added mass and fluid coupling with each structure. If the surrounding fluid was air, hydrodynamic forces could be neglected because of the low density. The pressure wave and fluid flow induced by turbulence in the water pipe system caused the vibration of the nuclear rod bundles as well as pressure scattering.

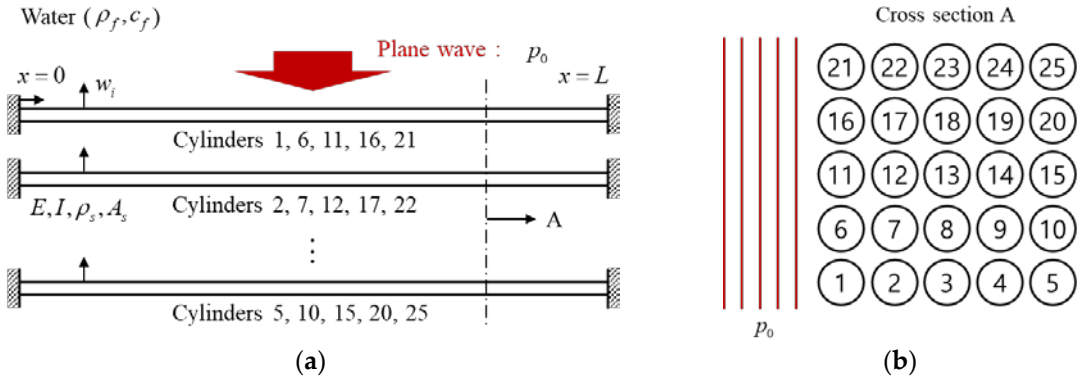

Figure 2. Nuclear fuel rod bundles consisting of 25 cylinders: (a) schematics and (b) cross section A.

2.2. Flexural Vibration of Nuclear Rod Bundles

To calculate the viscous hydrodynamic force acting on the nuclear rod bundles, the bi–Helmholtz equation using the linearized Navier–Stokes equation and continuity equations of the surrounding unbounded fluid for its structures presented in Figure 3 were obtained, as [1]

$$\nabla^2\left(\nabla^2 + k_v^2\right)\varphi = 0, \tag{2}$$

where φ is the streamline, k_v is the viscous wavenumber $k_v = (1 + \mathrm{i})\sqrt{\omega/2v}$, v is the kinematic viscosity of the fluid, and ω is the radial frequency variable. From Equation (2), we obtain the streamline φ_i of the surrounding fluid for cylinder i using

$$\varphi^i = \varphi_1^i + \varphi_2^i, \varphi_1^i = \sum_{i=1}^{N}\sum_{n=1}^{\infty}\left\{C_{n,i}^1 r_i^{-n}\cos n\theta + C_{n,i}^2 r_i^{-n}\sin n\theta\right\}, \varphi_2^i = \sum_{i=1}^{N}\sum_{n=1}^{\infty} C_{n,i}^3 H_n^{(1)}(kr_i)e^{\mathrm{i}n\theta}, \tag{3}$$

where $H_n^{(1)}$ is the Hankel function of the first kind and constants $C_{n,i}$ are determined from the boundary conditions. The boundary conditions were applied, as

$$\frac{1}{r}\frac{\partial\varphi}{\partial\theta_i}\bigg|_{r_i=R_i} = 0,\ i = 1, 2, \cdots, N,\ i \neq l; \tag{4}$$

$$\frac{1}{r}\frac{\partial\varphi}{\partial\theta_i}\bigg|_{r_i=R_i} = \dot{w}_l\cos\theta_l, \tag{5}$$

for $l = 1, 2, 3, \ldots, N$, where R_l is the radius of cylinder l, and $\dot{w}_l$ is the velocity of cylinder l, as shown in Figure 3. The viscous hydrodynamic forces on cylinder i are

$$F_{v,i} = -\mathrm{i}\omega e^{-\mathrm{i}\omega t}\rho_f R_i\int_0^{2\pi}\left[r_i\frac{\partial\varphi_1^i}{\partial r_i} + \varphi_2^i\right]\sin\theta_i d\theta_i, \tag{6}$$

where ρ_f is the fluid density. Substituting Equation (6) into (4) and (5), the viscous hydrodynamic forces were rewritten, as

$$F_{v,i} = -\rho_f\pi R_i^2\sum_{l=1}^{N}\alpha_{i,l}\ddot{w}_l, \tag{7}$$

where $\alpha_{i,l}$ is the dimensionless added mass of cylinder i from the vibration of cylinder l. To determine the dimensionless added mass $\alpha_{i,l}$, added mass $M_{i,l}$ was obtained by

$$M_{i,l} = \rho_f\pi R_i^2\alpha_{i,l}. \tag{8}$$

When $i = l$, added mass acts as the inertia loading to the cylinder vibration. The fluid coupling between the cylinders was analyzed similar to the influences by coupled viscoelastic spring. One cylinder vibration induced coupling to those of adjacent cylinders. The imaginary part of the added mass acts as the viscous damping. The vibration of cylinders coupled with viscous fluid induced a phase difference. The viscosity of fluid coupling improves the damping effect for the behaviors of nuclear rod bundles.

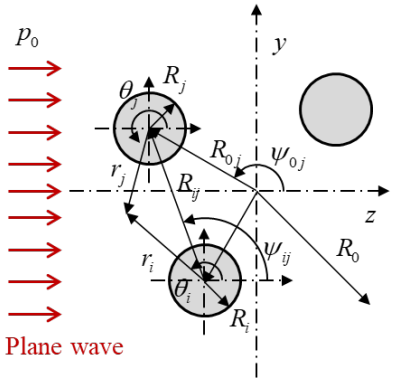

Figure 3. Definition diagram, coordinate systems and symbols used in the determination of the streamline and pressure of the surrounding fluid of the cylinders.

2.3. External Force Induced by the Pressure Wave

The pressure wave that was generated by the turbulent flow in the nuclear power reactors and the impacts of the external force were assumed to be of impulsive plane wave [20–22]. It is difficult to predict the magnitude of the pressure wave in real operating condition. Therefore, by calculating the transfer function of nuclear rod bundles applied to the pressure wave, the structural vibration can be simply predicted. When the pressure wave arrived at the nuclear rod bundles that consisted of multiple cylinders, the scattered wave interacted with the boundary surfaces of the structures. A multiple scattering analysis that was based on superposition using Graf's addition theorem was assumed [23]. After considering the interactions between the incident wave and the scattered waves from each cylinder, the total pressure in the unbounded fluid was expressed as

$$p(r,\theta_i) = \sum_{n=-\infty}^{\infty}\left[p_0 e^{-ik_f\gamma} i^n J_n(k_f r_i)e^{in\theta_i} + D_{n,i}H_n^{(1)}(k_f r_i)e^{in\theta_i} + \sum_{\substack{j=1 \\ j\neq i}}^{K} D_{n,j}\sum_{n=-\infty}^{\infty} H_{n-m}^{(1)}(k_f R_{ij})e^{i(n-m)\psi_{ij}} J_m(k_f r_i)e^{im\theta_i}\right], \; r_i < R_i, \quad (9)$$

where p_0 is the pressure of the incident traveling wave, γ is the start position of the wave, J_n is the Bessel function of the first kind, and constants D_n are determined from the boundary conditions. The boundary conditions at the cylinder wall were used to obtain the unknown coefficients in Equation (9). For each surrounding cylinder, the wall pressure conditions are given as

$$\left.\frac{\partial p}{\partial r_i}\right|_{r_i=R_i} = 0, \; i = 1,2,\cdots,N. \quad (10)$$

In order to simulate the scattering induced by the incident wave, the external forces from the incident wave and scattered waves were calculated as

$$F_{p,i} = \int_0^{2\pi} \left. p^i \right|_{r_i=R_i} R_i \cos\theta_i d\theta_i. \quad (11)$$

2.4. Numerical Model of Nuclear Rod Bundles

Flexural wave propagations were calculated using SEM to evaluate the structural instability of nuclear rod bundles in the fluid medium. The spectral element equation of the weak form based on a weighted–integral statement was derived. An eigenvalue problem was solved to determine the wavenumber of the flexural wave for the nuclear rod bundles in the fluid medium. The effects of added mass and fluid damping were investigated by changing the number of structures. The transfer function of the flexural vibration that was induced by incident pressure wave was calculated to evaluate the structural instability of the nuclear rod bundles.

Deriving the dynamic shape functions depended on the frequency domain, and the general solution of Equation (1) was assumed as

$$w_i(x,t) = \beta_i C e^{-\mathrm{i}kx} e^{\mathrm{i}\omega t}, \tag{12}$$

where β is the proportional coefficient for each general solution and k is the wavenumber. Substituting Equation (1) into (12), the eigenvalue problem was obtained by

$$(k^4 EI\mathbf{I} - \omega^2(\rho_s A_s \mathbf{I} + \mathbf{M}_a))\boldsymbol{\beta} = 0, \tag{13}$$

where $\mathbf{I}$ is the unit matrix of N by N, $\boldsymbol{\beta} = \begin{Bmatrix} \beta_1 & \beta_2 & \cdots & \beta_N \end{Bmatrix}^T$ and $\mathbf{M}_a$ is the matrix of added masses as

$$\mathbf{M}_a = \begin{bmatrix} M_{1,1} & M_{1,2} & \cdots & M_{1,N} \\ M_{2,1} & M_{2,2} & & M_{2,N} \\ \vdots & & \ddots & \vdots \\ M_{N,1} & M_{N,2} & \cdots & M_{N,N} \end{bmatrix}.$$

Equation (13) was rewritten in a linearized form by

$$\mathbf{C}\mathbf{x} = k\mathbf{J}\mathbf{x}, \tag{14}$$

where

$$\mathbf{x} = \begin{Bmatrix} \boldsymbol{\beta}^T & k\boldsymbol{\beta}^T & k^2\boldsymbol{\beta}^T & k^3\boldsymbol{\beta}^T \end{Bmatrix}^T,$$

$$\mathbf{C} = \begin{bmatrix} 0 & \mathbf{I} & 0 & 0 \\ 0 & 0 & \mathbf{I} & 0 \\ 0 & 0 & 0 & \mathbf{I} \\ \omega^2(\rho_s A_s \mathbf{I} + \mathbf{M}_a) & 0 & 0 & 0 \end{bmatrix},$$

and

$$\mathbf{J} = \begin{bmatrix} \mathbf{I} & 0 & 0 & 0 \\ 0 & \mathbf{I} & 0 & 0 \\ 0 & 0 & \mathbf{I} & 0 \\ 0 & 0 & 0 & EI\mathbf{I} \end{bmatrix}.$$

After the QR algorithm was applied to numerically solve Equation (14) using MATLAB, $4N$ wavenumbers k_i, proportional coefficients β_i determined by the material properties and frequency were obtained. While using the $4N$ wavenumbers, the general solutions of Equation (1) were obtained as

$$W_i(x) = \mathbf{e}(x,\omega)\mathbf{B}_i(\omega)\mathbf{a}, \tag{15}$$

where

$$\mathbf{e}(x,\omega) = \begin{Bmatrix} e^{-\mathrm{i}k_1 x} & e^{-\mathrm{i}k_2 x} & e^{-\mathrm{i}k_3 x} & \cdots & e^{-\mathrm{i}k_{4N} x} \end{Bmatrix}^T,$$

$$\mathbf{a} = \begin{Bmatrix} a_1 & a_2 & a_3 & \cdots & a_{4N} \end{Bmatrix}^T,$$

and

$$\mathbf{B}_i(\omega) = \begin{bmatrix} \beta_{i,1} & & & \\ & \beta_{i,2} & & \\ & & \ddots & \\ & & & \beta_{i,4N} \end{bmatrix}.$$

The spectral nodal displacement of the multiple-beam element in the flexural direction is expressed by

$$\mathbf{d} = \left\{ \begin{array}{cccccccccc} W_1(0) & W'_1(0) & \cdots & W_N(0) & W'_N(0) & W_1(L) & W'_1(L) & \cdots & W_N(L) & W'_N(L) \end{array} \right\}^T. \quad (16)$$

Substituting Equation (15) into (16),

$$\mathbf{d} = \mathbf{H}(\omega)\mathbf{a}, \quad (17)$$

where

$$\mathbf{H}(\omega) = \begin{bmatrix} \beta_{1,1} & \beta_{1,2} & \cdots & \beta_{1,4N} \\ -\mathrm{i}k_1\beta_{1,1} & -\mathrm{i}k_2\beta_{1,2} & & -\mathrm{i}k_{4N}\beta_{1,4N} \\ \vdots & \vdots & & \vdots \\ \beta_{4N,1} & \beta_{4N,2} & & \beta_{4N,4N} \\ -\mathrm{i}k_1\beta_{4N,1} & -\mathrm{i}k_2\beta_{4N,2} & \cdots & -\mathrm{i}k_{4N}\beta_{4N,4N} \\ \beta_{1,1}e^{-\mathrm{i}k_1\beta_{1,1}L} & \beta_{1,2}e^{-\mathrm{i}k_2\beta_{1,2}L} & \cdots & \beta_{1,4N}e^{-\mathrm{i}k_{4N}\beta_{1,4N}L} \\ -\mathrm{i}k_1\beta_{1,1}e^{-\mathrm{i}k_1\beta_{1,1}L} & -\mathrm{i}k_2\beta_{1,2}e^{-\mathrm{i}k_2\beta_{1,2}L} & & -\mathrm{i}k_{4N}\beta_{1,4N}e^{-\mathrm{i}k_{4N}\beta_{1,4N}L} \\ \vdots & \vdots & & \vdots \\ \beta_{4N,1}e^{-\mathrm{i}k_1\beta_{4N,1}L} & \beta_{4N,2}e^{-\mathrm{i}k_2\beta_{4N,2}L} & & \beta_{4N,4N}e^{-\mathrm{i}k_{4N}\beta_{4N,4N}L} \\ -\mathrm{i}k_1\beta_{4N,1}e^{-\mathrm{i}k_1\beta_{4N,1}L} & -\mathrm{i}k_2\beta_{4N,2}e^{-\mathrm{i}k_2\beta_{4N,2}L} & \cdots & -\mathrm{i}k_{4N}\beta_{4N,4N}e^{-\mathrm{i}k_{4N}\beta_{4N,4N}L} \end{bmatrix}.$$

Using Equations (15) and (17), the flexural vibrations of the nuclear rod bundles in terms of the nodal displacement were obtained by

$$W_i(x) = \mathbf{N}_{w,i}(x,\omega)\mathbf{d}, \quad (18)$$

where $\mathbf{N}_{w,i}(x,\omega) = \mathbf{e}(x,\omega)\mathbf{B}_i\mathbf{H}^{-1}(\omega)$. In order to obtain the spectral element equations for Equation (1), the weak form was derived from the weighted–integral statement by

$$\int_0^L \left[\sum_{i=1}^{4N} \left\{ EIW''_i\delta W''_i - \omega^2\rho_s A_s W_i\delta W_i - \omega^2 \sum_{j=1}^{4N} M_{i,j}W_j\delta W_j - F_{i,2}\delta W_i \right\} \right] dx = \sum_{i=1}^{4N} F_{W,i}(x)\delta W_i \Big|_0^L + \sum_{i=1}^{4N} F_{\Theta,i}(x)\delta W'_i \Big|_0^L, \quad (19)$$

where δW is the arbitrary variation in W, and $F_{W,i}$ and $F_{\Theta,i}$ are the transverse shear force and bending moment, respectively, as

$$F_{W,i}(x) = -EI\frac{\partial^3 W_i(x)}{\partial x^3},$$

$$F_{\Theta,i}(x) = EI\frac{\partial^2 W_i(x)}{\partial x^2}.$$

Substituting Equation (18) into (19), the spectral element equation was obtained, as

$$\mathbf{S}(\omega)\mathbf{d} = \mathbf{f}(\omega) + \mathbf{f}_2(\omega), \quad (20)$$

where $\mathbf{S}$ is the symmetric spectral element matrix for the flexural vibration of the nuclear rod bundles in the fluid as

$$\mathbf{S}(\omega) = \mathbf{H}^{-T}\left(\sum_{i=1}^{N} \left(EI\mathbf{B}_i\mathbf{K}^2\mathbf{E}\mathbf{K}^2\mathbf{B}_i - \rho_s A_s\omega^2\mathbf{B}_i\mathbf{E}\mathbf{B}_i - \omega^2 \sum_{j=1}^{N} M_{i,j}\mathbf{B}_i\mathbf{E}\mathbf{B}_j \right) \right)\mathbf{H}^{-1}.$$

Here, $\mathbf{E}(\omega) = \int_0^L \mathbf{e}^T(x,\omega)\mathbf{e}(x,\omega)dx$ and $\mathbf{K}$ is the wavenumber matrix as

$$\mathbf{K}^2 = \begin{bmatrix} k_1^2 & & & \\ & k_2^2 & & \\ & & \ddots & \\ & & & k_{4N}^2 \end{bmatrix}.$$

$\mathbf{f}$ is the spectral nodal force component for the beam element given as

$$\mathbf{f}(\omega) = \begin{Bmatrix} \mathbf{f}_b(0,\omega) \\ \mathbf{f}_b(L,\omega) \end{Bmatrix},$$

where $\mathbf{f}_b(x,\omega) = \begin{Bmatrix} F_{W,1}(x,\omega) & F_{\Theta,1}(x,\omega) & \cdots & F_{W,N}(x,\omega) & F_{\Theta,N}(x,\omega) \end{Bmatrix}^T$, and $\mathbf{f}_2$ is the spectral nodal force component induced by the pressure wave, as

$$\mathbf{f}_2(\omega) = \int_0^L \sum_{i=1}^{N} F_{i,2}(\omega)\mathbf{N}_{w,j}^T(x,\omega)dx.$$

3. Results and Discussion

When considering the single cylinder in the presence of an inviscid fluid, the dimensionless added mass α is equal to one, regardless of the vibrating frequencies. For a single cylinder in viscous fluid, the exact dimensionless added mass was calculated as [24]

$$\alpha_{\text{ext}} = 1 + \frac{4\text{i}K_1(-\text{i}\sqrt{\text{iRe}})}{\sqrt{\text{iRe}}K_0(-\text{i}\sqrt{\text{iRe}})}, \tag{21}$$

where K_0 and K_1 are the modified Bessel functions of the third kind, and Re = $\rho_f \omega R_2/\mu$. The dimensionless added mass of a single cylinder in the fluid medium was calculated, as shown in Figure 4. The radius of the cylindrical beam R was 0.005 m. The fluid was assumed to be water, at 4 °C (ρ_f = 1,000 kg/m^3 and μ = 1.519 × 10-3 Ns/m^2). When compared with Lin's method, the results of the exact solution (Figure 3) were in good agreement. The dimensionless added masses of the 25 cylinders were calculated using Lin's method presented in Figure 5. The gap between each cylinder was 0.001 m. The start position of the traveling wave is 0.05 m. As the number of cylinders increased, the added mass and fluid damping also increased due to more interactions between the multiple cylinders. The fluid coupling effects became significant when the structures were concentrated.

Figure 6 shows the real part of the pressure that was obtained for propagating plane waves. The scattering is more significant when the frequency of the incident wave is larger. The increasing number of cylinders induced more significant scattering.

Figure 7 shows the external forces from the unit pressure of the incident wave. The external forces were proportional to the input frequency of the incident wave. The forces acting on cylinders 1, 6, 11, 16, and 21 were higher than those acting on other cylinders. The external forces acting on cylinders located outside of the complex structures were influenced by the instability of the nuclear rod bundles in the fluid.

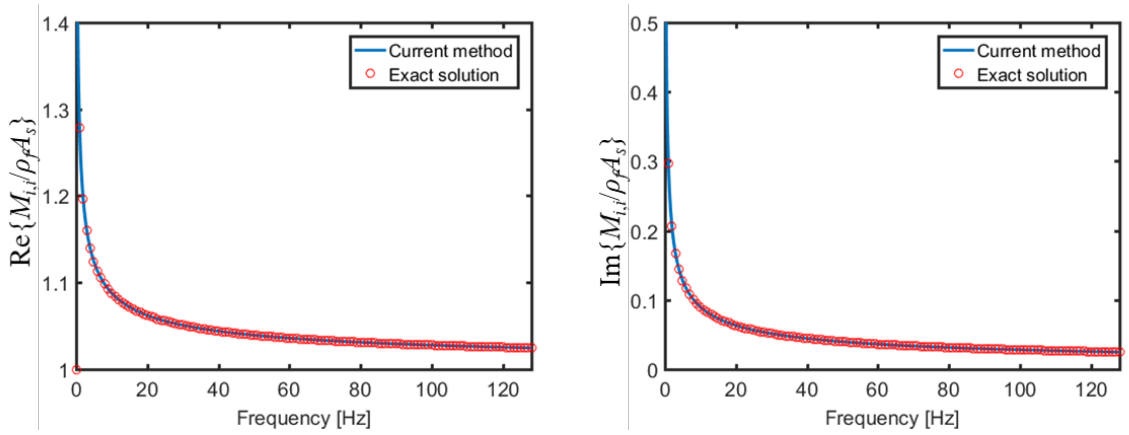

Figure 4. Comparison between exact solutions and calculated added masses of a single cylinder using Lin's method: (**a**) real part and (**b**) imaginary part.

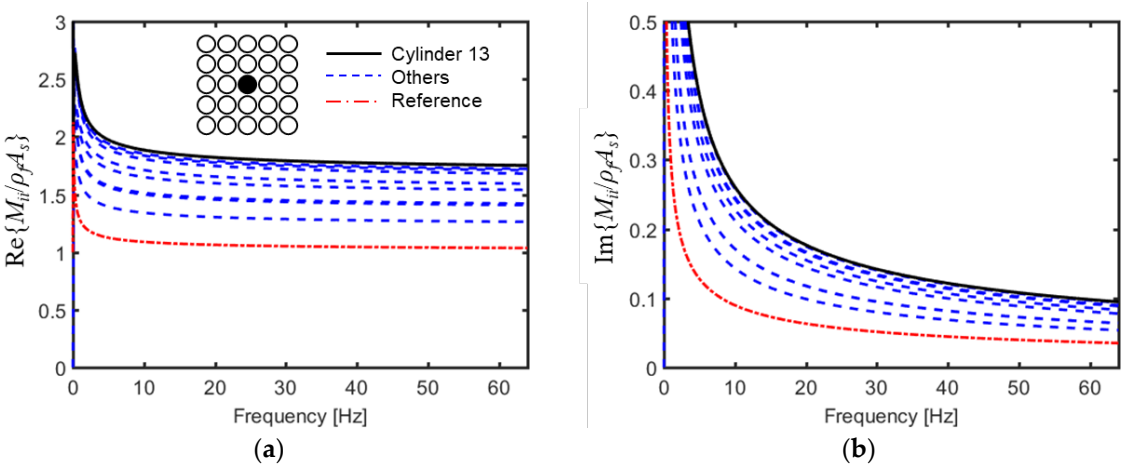

Figure 5. Calculated added comparison between exact solutions and calculated added masses of a single cylinder using Lin's method: (**a**) real part and (**b**) imaginary part.

The point force was applied to the fixed beam, as shown in Figure 8a. The displacement responses for the flexural vibration of a single cylindrical beam in the fluid medium were predicted, as shown in Figure 8b,c. The single cylindrical beam without water vibrated having not a time decay. Fluid damping did not occur without the presence of water, and only structural damping influenced vibration. Otherwise, the vibration magnitude of cylindrical beam considering the added mass and fluid coupling induced fast decay in comparison with only structural damping. The application of the added mass increased the total damping because of the viscous effects. The increased decay in the predicted responses was observed when the beam was placed in the water.

The impact response of the nuclear rod bundles consisting of multiple cylinders was predicted, as shown in Figure 9. The resonant response of the nuclear rod bundles consisting of multiple cylinders occurred at lower frequencies. When the number of cylindrical beams N increased, the total damping of nuclear rod bundles also increased. The fluid coupling that was caused by the viscous damping of the fluid gaps between each structure was increased when the number of cylindrical beam increased. The fluid damping increased in the presence of surrounding structures due to small gaps between the vibrating structures.

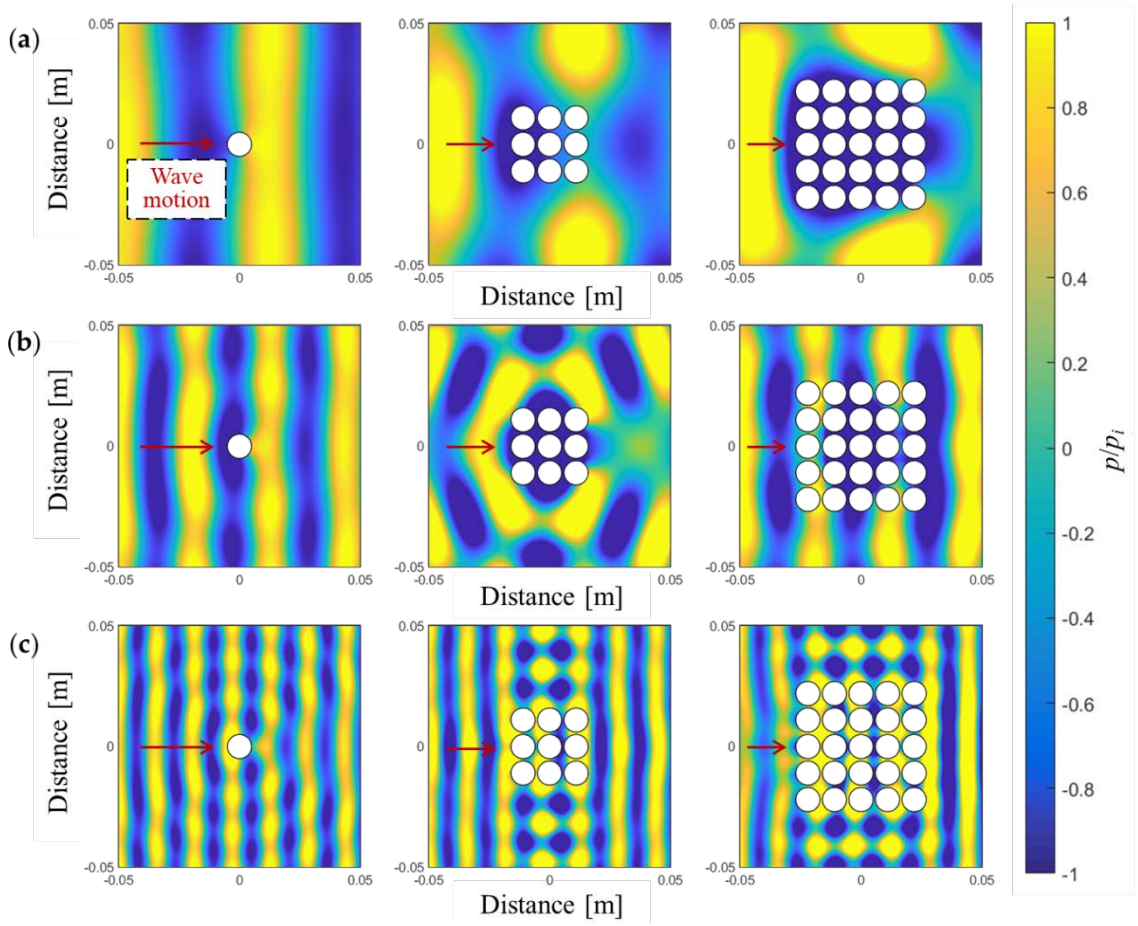

Figure 6. Pressure wave pattern produced by the multiple scattering of the plane wave with a wavelength of (**a**) k_fR = 0.5, (**b**) k_fR = 1.0, and (**c**) k_fR = 2.0. The left, middle, and right sides of the contours represent wave propagation with one, nine, and 25 cylinders.

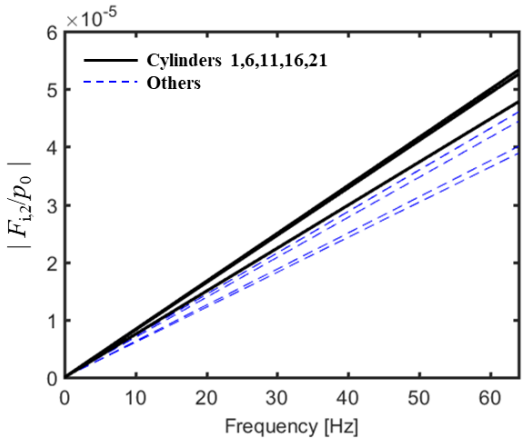

Figure 7. Amplitudes of pressure forces acting on the multiple cylinders caused by pressure scattering wave.

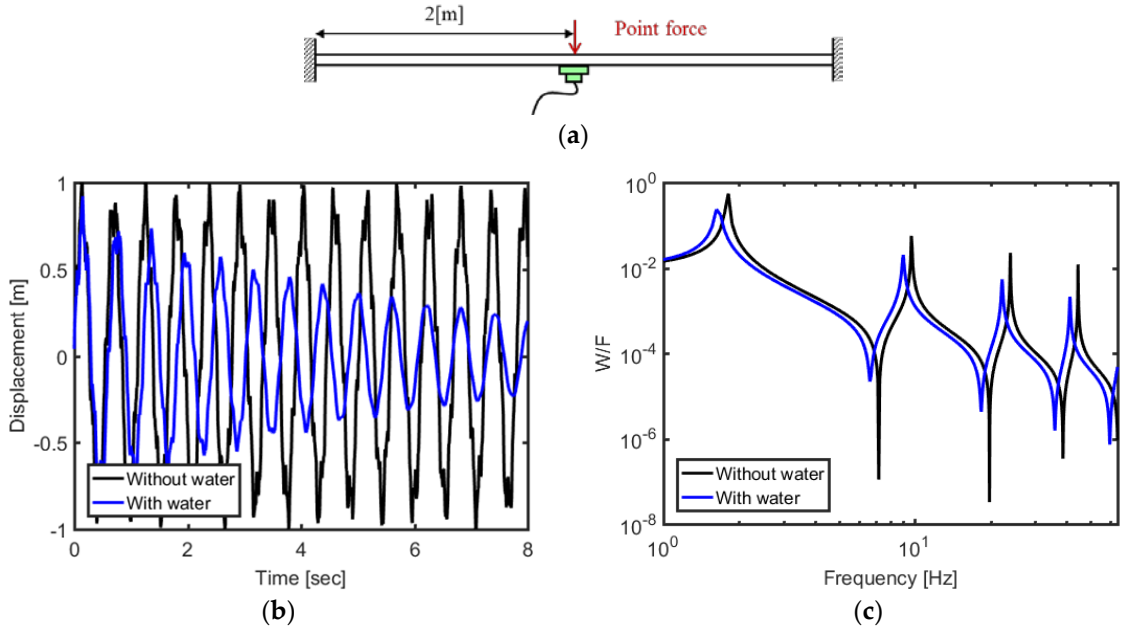

Figure 8. Fluid effects of flexural vibration of a single cylindrical beam in the fluid: (**a**) dynamic model of fixed–fixed beam; (**b**) flexural displacement; and, (**c**) frequency response function.

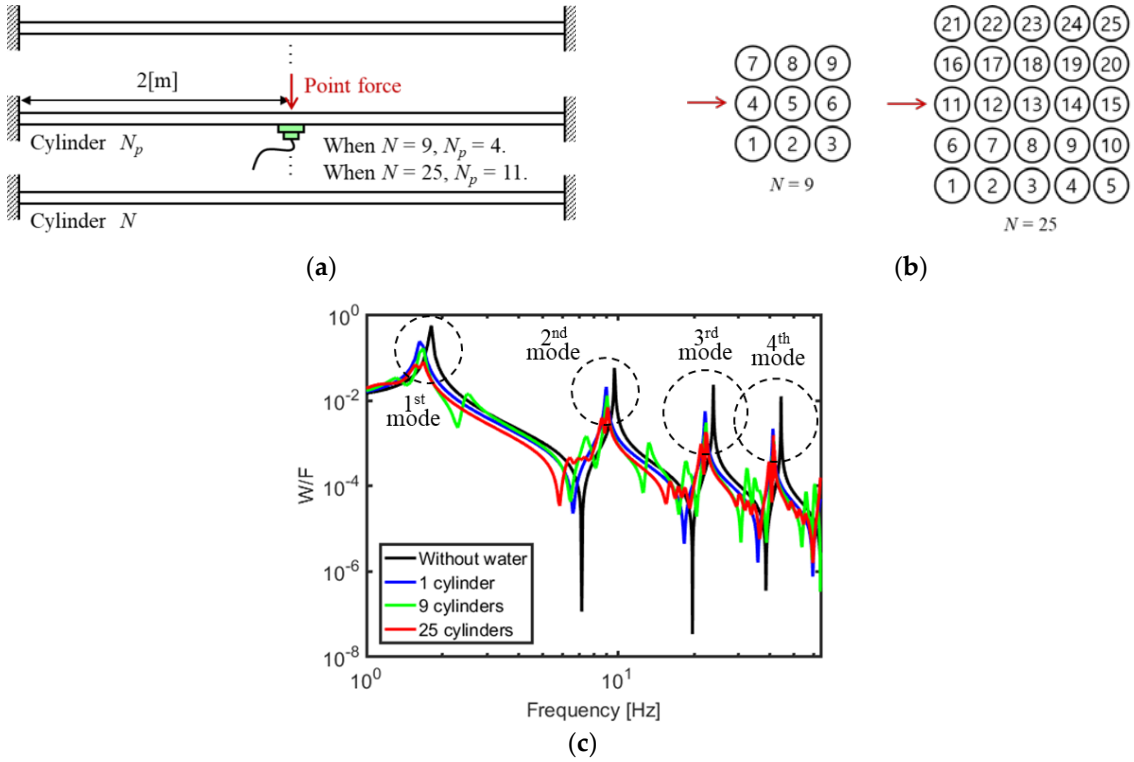

Figure 9. (**a**) Nuclear fuel rod bundles varying the number of cylinders in the fluid subjected to point force, (**b**) cross section, and (**c**) calculated transfer functions.

The modes shapes of the nuclear rod bundles in the fluid medium were predicted to confirm the viscous fluid in the gaps between each multiple cylinders, as shown in Figure 10. The mode for each cylindrical beams overlapped with modes of other cylindrical beams, depending on the number of cylinders, but in various phases. The complex structure with nine cylinders had nine overlapping modes and the complex structure with 25 cylinders had 25 overlapping modes. When the number of

the cylindrical beams increased, the interacted surface areas became larger. Moreover, the different phases of the cylindrical beams caused the reaction of mass coupling of each cylinders having viscous effects. The effective damping increased with the increase in number of cylinders.

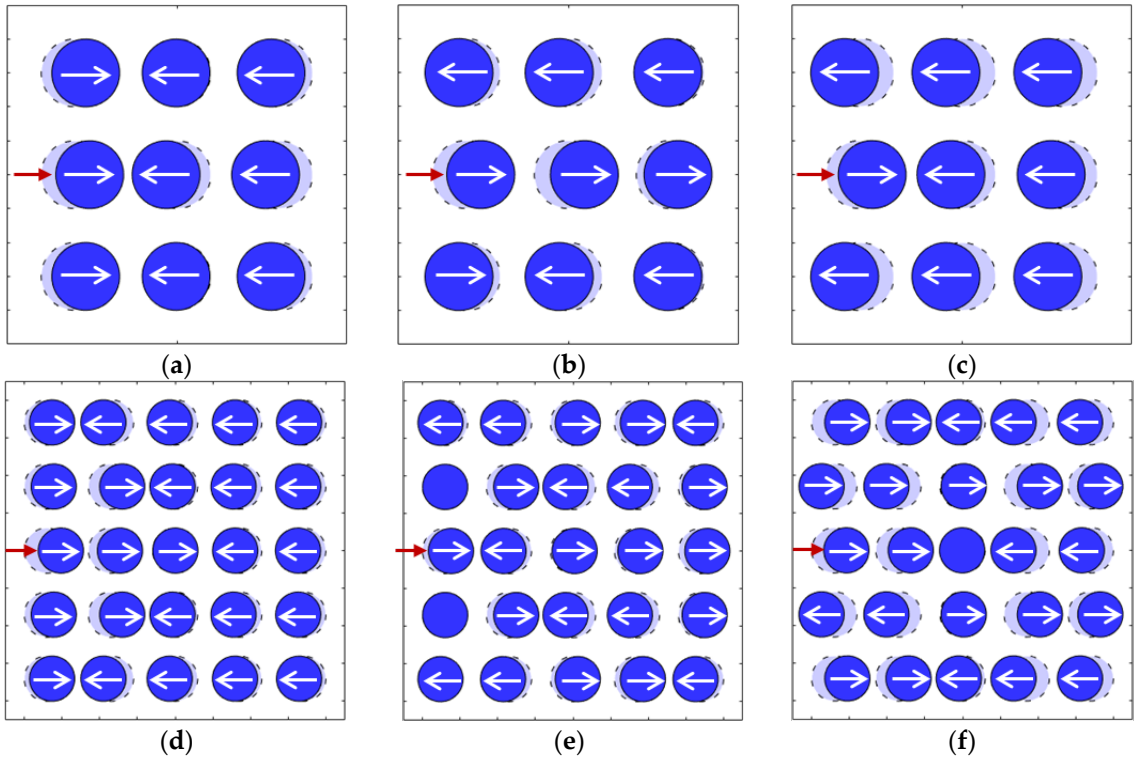

Figure 10. Mode shapes of nuclear fuel rod bundles in the fluid medium: (**a**) $N = 9, f = 1.3$ Hz; (**b**) 1.6 Hz; (**c**) 2.5 Hz; (**d**) $N = 25, f = 1.1$ Hz; (**e**) 1.6 Hz; and, (**f**) 9.1 Hz.

Figure 11 shows the calculated transfer functions for the nuclear rod bundles that consisted of multiple cylinders that were subjected to a pressure wave together with its first mode shape. When the propagating pressure was acting on the nuclear rod bundles, viscous damping was insignificant because the phases of all the beams were identical. In the case of water, the wavelength at the frequency of 100 Hz is 44.8 m. The wavelength in water is larger than the distance between the cylinders in the low frequency range. The distances between cylinders were identical. Thus, the fluid couplings induced negligible viscous effects to the vibrating structures. The phase difference of the structures caused the viscous fluid damping to increase. When the distance of each fuel rods is smaller than the cross-sectional dimensions, the fluid coupling that causes the vibration modes in viscous fluid medium is more important.

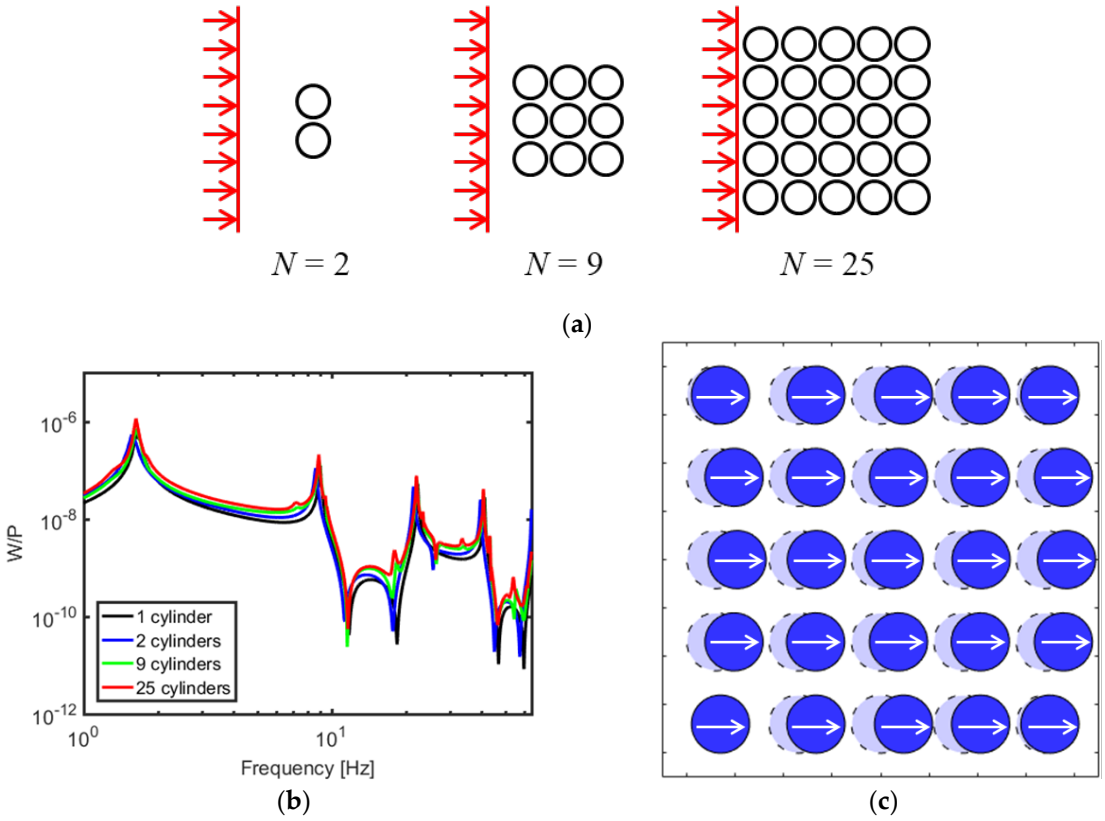

Figure 11. (**a**) Calculated transfer functions for nuclear fuel rod bundles varying the number of cylinders subjected to pressure wave, (**b**) cross section, and (**c**) its first mode shape at $N = 25$ and $f = 1.6$ Hz.

4. Conclusions

The structural vibration of nuclear rod bundles that are induced by propagating pressure waves was simulated by using SEM. Added mass and fluid coupling of the surrounding fluid were calculated using the viscous fluid theory to investigate the fluid forces acting on the nuclear rod bundles in the viscous fluid. The external forces that were caused by the incident wave and scattering pressure fields were predicted from the solution of the acoustic wave equation. The spectral element equation for the flexural vibration of nuclear rod bundles in the fluid medium subjected to external force was derived while using the weighted–integral statement. The structural damping of nuclear rod bundles in the fluid medium increased due to viscous effects in the mass coupling. Furthermore, the natural frequency of the nuclear rod bundles was decreased by the added mass. When the number of cylinders increased, the total damping also increased, because the number of the viscous fluid coupling dissipating the vibration energy was larger. The flexural vibrations of the nuclear rod bundles that were induced by the propagating pressure wave exhibited smaller damping due to same phase responses of each cylindrical beam. When the wavelength was longer than the gaps of the nuclear rod bundles, the effective damping of the underwater structure tended to decrease. The proposed method can be utilized for designing the underwater structure of the nuclear rod bundles, water pipe systems, and vessels conveying fluid, as well as the development of damping treatment for the reduction of vibration induced by the fluid effect.

Author Contributions: Conceptualization, W.Y., H.K., and J.P.; Data curation, W.Y.; Formal analysis, W.Y.; Investigation, W.Y.; Methodology, W.Y.; Project administration, H.K. and J.P.; Resources, H.K.; Software, W.Y.; Supervision, J.P.; Validation, W.Y.; Writing—original draft, W.Y.; Writing—review and editing, W.Y., H.K., and J.P. All authors have read and agreed to the published version of the manuscript.

Funding: This work was supported by the National Research Foundation of Korea(NRF) grant funded by the Korea government(MSIT) (No. 2019R1G1A1097252).

Conflicts of Interest: The authors declare no conflict of interest.

References

1. Païdoussis, M.P. *Fluid–Structure Interactions: Slender Structures and Axial Flow*, 2nd ed.; Academic Press: Oxford, UK, 2014; Volume 1.
2. Doaré, O.; Langre, E. Local and global instability of fluid–conveying pipes on elastic foundations. *J. Fluids Struct.* **2002**, *16*, 1–14. [CrossRef]
3. Païdoussis, M.P.; Issid, N. Dynamic stability of pipes conveying fluid. *J. Sound Vib.* **1974**, *33*, 267–294. [CrossRef]
4. Kim, T.; Je, S.; Chang, Y. Fluid−elastic instability evaluation for reactor vessel internals with structural interaction. *Prog. Nucl. Energy* **2019**, *110*, 41–50. [CrossRef]
5. Lu, J.; Yuan, S.; Parameswaran, S.; Yuan, J.; Ren, X.; Si, Q. Investigation on the vibration and flow instabilities induced by cavitation in a centrifugal pump. *Adv. Mech. Eng.* **2017**, *9*, 1–11. [CrossRef]
6. Ferrari, G.; Balasubramanian, P.; Guisquet, S.; Piccagli, L.; Karazis, K.; Painter, B.; Amabili, M. Non linear vibrations of nuclear fuel rods. *Nucl. Eng. Des.* **2018**, *338*, 269–283. [CrossRef]
7. Choi, M.; Kang, H.; Yoon, K.; Song, K. Vibration analysis of a dummy fuel rod continuously supported by spacer grids. *Nucl. Eng. Des.* **2004**, *232*, 185–196. [CrossRef]
8. Lee, Y.; Kim, H. Effect of spring shapes on the variation of loading conditions and the wear behavior of the nuclear fuel rod during fretting wear tests. *Wear* **2007**, *263*, 451–457. [CrossRef]
9. Wiggert, D.C.; Tijsseling, A.S. Fluid transients and fluid–structure interaction in flexible liquid–filled piping. *Appl. Mech. Rev.* **2001**, *54*, 455–481. [CrossRef]
10. Sreejith, B.; Jayaraj, K.; Ganesan, N.; Padmanabhan, C.; Chellapandi, P.; Selvaraj, P. Finite element analysis of fluid–structure interaction in pipeline systems. *Nucl. Eng. Des.* **2004**, *227*, 313–322. [CrossRef]
11. Bazilevs, Y.; Calo, V.M.; Zhang, Y.; Hughes, T.J.R. Isogeometric fluid–structure interaction analysis with applications to arterial blood flow. *Comput. Mech.* **2006**, *38*, 310–322. [CrossRef]
12. Strang, G. *Computational Science and Engineering*; Wellesley–Cambridge Press: Wellesley, MA, USA, 2007.
13. Cook, R.D. *Concepts and Applications of Finite Element Analysis*; John Wiley and Sons: New York, NY, USA, 2007.
14. Lee, U. *Spectral Element Method in Structural Dynamics*; John Wiley and Sons: Singapore, 2009.
15. Lee, U.; Oh, H. The spectral element model for pipelines conveying internal steady flow. *Eng. Struct.* **2003**, *25*, 1045–1055. [CrossRef]
16. Lee, U.; Park, J. Spectral element modelling and analysis of a pipeline conveying internal unsteady fluid. *J. Fluids Struct.* **2006**, *22*, 273–292. [CrossRef]
17. Lee, U.; Jang, I. Spectral element modeling and analysis of the blood flows in viscoelastic vessels. *Appl. Math. Comput.* **2012**, *218*, 7295–7307. [CrossRef]
18. Kjolsing, E.J.; Todd, M.D. Frequency response of a fixed–fixed pipe immersed in viscous fluids, conveying internal steady flow. *J. Pet. Sci. Eng.* **2015**, *134*, 247–256. [CrossRef]
19. Kjolsing, E.J.; Todd, M.D. Damping of a fluid–conveying pipe surrounded by a viscous annulus fluid. *J. Sound Vib.* **2017**, *394*, 575–592. [CrossRef]
20. Wu, J.M.; Liang, H.Y.; Zhu, F.J.; Lei, J. CFD analysis of the impact of a novel spacer grid with longitudinal vortex generators on the sub-channel flow and heat transfer of a rod bundle. *Nucl. Eng. Des.* **2017**, *324*, 78–92. [CrossRef]
21. Mohany, A.; Hassan, M. Modelling of fuel bundle vibration and the associated fretting wear in a CANDU fuel channel. *Nucl. Eng. Des.* **2013**, *264*, 214–222. [CrossRef]
22. Tian, W.X.; Zhang, K.; Hou, Y.D.; Zhang, Y.P.; Qiu, S.Z.; Su, G.H. Hydrodynamics of two-phase flow in a rod bundle under cross-flow condition. *Ann. Nucl. Eng.* **2016**, *91*, 206–214. [CrossRef]
23. Cho, S.; Yang, W.; Lee, S.; Park, J. Flexural wave cloaking via embedded cylinders with systematically varying thicknesses. *J. Acoust. Soc. Am.* **2016**, *139*, 3320–3324. [CrossRef] [PubMed]

24. Sader, J.E. Frequency response of cantilever beams immersed in viscous fluids with applications to the atomic force microscope. *J. Appl. Phys.* **1998**, *84*, 64. [CrossRef]